Biochemical and Biophysical Research Communications 433 (2013) 145–150

Contents lists available at SciVerse ScienceDirect

Biochemical and Biophysical Research Communications

journal homepage: www.elsevier.com/locate/ybbrc

Impaired energy metabolism in a *Drosophila* model of mitochondrial aconitase deficiency

Zhang Cheng [a], Manabu Tsuda [b], Yoshihito Kishita [a,c], Yukiko Sato [a], Toshiro Aigaki [a,*]

[a] Department of Biological Sciences, Tokyo Metropolitan University, 1-1 Minami-osawa, Hachioji, Tokyo 192-0397, Japan
[b] Faculty of Health and Social Services, Kanagawa University of Human Services, 1-10-1 Heisei-cho Yokosuka, Kanagawa 238-8522, Japan
[c] Division of Functional Genomics and Systems Medicine, Research Center for Genomic Medicine, Saitama Medical University, 1397-1 Yamane, Hidaka, Saitama 350-1241, Japan

ARTICLE INFO

Article history:
Received 11 February 2013
Available online 21 February 2013

Keywords:
Drosophila
Disease model
Mitochondrial aconitase
Metabolomics

ABSTRACT

Aconitase catalyzes the conversion of citrate to isocitrate in the tricarboxylic acid (TCA) cycle, and its deficiency in humans is associated with an infantile neurodegenerative disorder affecting mainly the cerebellum and retina. Here we investigated the effect of gene knockout and knockdown of the mitochondrial aconitase *Acon* in *Drosophila*. *Acon*-knockout flies were homozygous lethal, indicating that *Acon* is essential for viability. RNA interference-generated *Acon*-knockdown flies exhibited a variety of phenotypes, such as reduced locomotor activity, a shortened lifespan, and increased cell death in the developing brain. Metabolomic analysis revealed that acetyl-CoA, citrate/isocitrate, and *cis*-aconitate were significantly increased, while most metabolites of glycolysis and the TCA cycle were reduced. Reduced triacylglyceride and increased acetyl-CoA suggested that lipids were used as an energy source because of the impaired glycolysis and TCA cycle. The *Acon*-knockdown model should facilitate further understanding of the pathophysiology of *m*-aconitase deficiency in humans.

1. Introduction

The tricarboxylic acid (TCA) cycle is a series of enzymatic reactions that plays a fundamental role in aerobic respiration to produce ATP. Aconitase, an enzyme of the TCA cycle, catalyzes the stereo-specific isomerization of citrate to isocitrate via *cis*-aconitate [1–3]. In eukaryotes, there are two types of aconitase: mitochondrial aconitase (*m*-aconitase) and cytosolic aconitase (*c*-aconitase) [4]. *m*-Aconitase has two major functions: as an enzyme in the TCA cycle and as a biosensor for reactive oxygen species and iron [5–7]. Oxidative inactivation of *m*-aconitase in rat primary mesencephalic cultures results in neurotoxicity [6]. In addition, *m*-aconitase is a target of oxidative damage during aging [8–11].

In humans, *m*-aconitase deficiency causes a variety of symptoms. Patients with a point mutation in *ACO2* encoding *m*-aconitase exhibit truncal hypotonia, athetosis, seizure disorder, infantile cerebellar-retinal degeneration, and a short lifespan [12]. To gain further insight into the molecular pathophysiology of *m*-aconitase deficiency, it is crucial to establish an experimental animal model for this genetic defect. In this study, we investigated a *Drosophila* model of *m*-aconitase deficiency. Because knockout mutants are embryonic lethal, we used RNA interference (RNAi)-mediated knockdown to make flies with low *m*-aconitase activity (*Acon*-knockdown flies). *Acon*-knockdown flies showed reduced locomotor activity, a shortened lifespan, and increased cell death in the developing brain; these phenotypes are also observed in humans with defective *m*-aconitase. Metabolome analysis of *Acon*-knockdown flies revealed that glycolysis and the TCA cycle were clearly impaired, and ATP levels were significantly reduced. We also found that triacylglyceride levels greatly decreased within a few days. These data strongly suggest that lipids were used to produce energy via fatty acid oxidation. *Acon*-knockdown *Drosophila* should provide a useful model to understand the pathophysiology of *m*-aconitase deficiency in humans.

2. Materials and methods

2.1. Fly strains

Flies were reared at 25 °C on a standard glucose-yeast-agar media containing propionic acid and *n*-butyl *p*-hydroxybenzoate as mold inhibitors. *P*-element transposon insertion lines in the *Acon* locus: *P{PZ}Acon*^{07054}, *P{PZ}Acon*^{01705a}, *Mi{ET1}Acon*^{MB09176}, and *P{UAS-Acon.IR}*102 were obtained from the Bloomington *Drosophila* Stock Center (BDSC, Bloomington, IN). *act5c-GAL4* [13] flies were obtained from the *Drosophila* Genetic Resource Center (DGRC, Kyoto, Japan). RNAi lines targeting *Acon*, *{GD*1348*}v*11767 and *P{GD*1348*}v*12455, were from the Vienna *Drosophila* RNAi Center (VDRC, Vienna, Austria).

* Corresponding author. Fax: +81 42 677 2559.
E-mail address: aigaki-toshiro@tmu.ac.jp (T. Aigaki).

0006-291X/$ - see front matter © 2013 Elsevier Inc. All rights reserved.
http://dx.doi.org/10.1016/j.bbrc.2013.02.040

Acon-knockout ($Acon^{KO}$) flies were generated by the ends-out gene targeting technique as described previously [14]. To construct the targeting donor plasmid, approximately 2 kb-long homologous arms, corresponding to the upstream and downstream regions of the *Acon* locus, were amplified by PCR with the following primers: *Acon*-3′ (forward: 5′-GCGGCCGCGCAGGAACAGATATTTCGCTCATC-3′, reverse: 5′-ACTAGTTTGATTATCATGTCAAGAGGACGAG-3′) and *Acon*-5′ (forward: 5′-GGCCGGCCTGGTGTCAATTTGACTGGCAAGATC-3′, reverse: 5′-CTCGAGCAATTTCTCGCTATCGTTCGGCTAC-3′), respectively. The PCR-amplified fragments were subcloned into the polylinker of *p*{*EndOut2*} [15]. The mini-*white* gene was inserted between the upstream and downstream target sequences as a transformation marker. *Acon*-targeting construct *P*{*donor*} lines were generated by *P*-element-mediated transformation [16] using the y^1w^{67c23} strain as a recipient. 6935-hid and *w*; *Pin*/*CyO*; $Gal4^{221[w-]}$ flies (obtained from BDSC) were used for targeting crosses [15].

Transgenic flies carrying *UAS-Acon* were generated by ϕC31 integrase-mediated attB–attP transformation [17]. cDNA corresponding to the coding region of *Acon* was obtained by reverse transcription PCR (RT-PCR) using mRNAs isolated from adult *Drosophila*, and subcloned into pUASTattB [17] using the primers *Acon* cDNA forward (5′-AGATCTCAAAATGGCTGCGAGATTGATGAACG-3′) and *Acon* cDNA reverse (5′-CTCGAGTTACTGGGCCAGCTCCTTCATG-3′). The construct was injected into embryos. The *ZH-attP-86Fb* strain was used as a recipient [17]. All fly stocks, including the targeted lines and transgenic lines were backcrossed to the y^1w^{67c23} strain for six generations before use in experiments.

2.2. Quantitative real-time PCR

Total RNA was extracted from 3-day-old female flies using TRIzol reagent (Invitrogen, Carlsbad, CA) and reverse-transcribed using SuperScript III (Invitrogen). Quantitative RT-PCR was performed using SYBR Premix Ex Taq (TaKaRa, Ootsu, Japan) and the Chromo 4 Four-color Real-Time System (Bio-Rad, Hercules, CA). The expression levels were normalized to that of *rp*49. The primers used were *Acon* forward: 5′-AGAAGTTCAAGCTCAAGGCTCC-3′, *Acon* reverse: 5′-GACAGCCACCTTGACATTTTCG-3′, *rp*49 forward: 5′-GCTAAGCTGTCGCACAAATG-3′, and *rp*49 reverse: 5′-TGTGCACCAGGAACTTCTTG-3′.

2.3. Measurement of aconitase activity

m-Aconitase activity was measured using an Aconitase Assay Kit (Cayman Chemical Company, Ann Arbor, MI). Fifty flies were homogenized in 0.5 ml of the supplied homogenization buffer and centrifuged for 10 min at 800×*g* at 4 °C to remove debris. The supernatant was then spun for 10 min at 20,000×*g* at 4 °C to precipitate the mitochondrial fraction. The pellet was resuspended in 1 ml of homogenization buffer and sonicated for 20 s. Fifty microliters of the mitochondrial suspension were added to 100 μl of assay mixture and incubated for 15 min at 37 °C, protected from light. The reaction was initiated by adding 50 μl of diluted substrate solution, and the absorbance at 340 nm was monitored once a minute. Aconitase activity was calculated according to the manufacturer's protocol. Protein concentration was determined using Bio-Rad protein assay reagent. All measurements were performed in at least triplicate.

2.4. Measurement of metabolites

Ten females were collected and homogenized in 200 μl of 75% acetonitrile on ice. The homogenates were centrifuged for 10 min at 12,000×*g* to remove debris. The supernatant was dried in a miVac Sample Concentrator (Genevac, Stone Ridge, NY), and dissolved in 20 μl of 10 mM Dibutyl ammonium acetate (DBAA) (pH 4.95). The samples were analyzed using a liquid chromatography quadrupole time-of-flight mass spectrometry (LC-QTofMS) system, ACQUITY UPLC and Xevo QTofMS (Waters, Milford, MA). The separation was carried out on an ACQUITY UPLC HSS T3 column (2.1 × 100 mM, 1.8 μM; Waters) by a gradient of mobile phase from 10 mM DBAA to 100% acetonitrile over a 20 min run. The MS system was equipped with dual electrospray ionization (ESI) probe and operated in the negative ion mode. The data were analyzed using MarkerLynx™ and QuanLynx™(Waters). Compounds were identified based on the retention time, *m*/*z* ratio, and MS/MS spectrum.

2.5. Measurement of CO_2 production and ATP content

The production of CO_2 was measured as described [18]. Assays were performed at least five times for each genotype. For measurement of ATP content, fifteen adult flies were homogenized in 200 μl of 6 M guanidine hydrochloride, incubated for 5 min at 95 °C, and then centrifuged for 5 min at 17,000×*g* at 4 °C. The supernatant was diluted 1000-fold with TE (pH 8.0). ATP was measured using an ATP bioluminescent assay determination kit (Sigma–Aldrich, St. Louis, MO). ATP concentration was normalized to protein concentration.

2.6. Nile red staining and triacylglyceride measurement

Fat bodies were dissected from the abdomens of 1- or 3-day-old female flies, and mounted in 0.00025% Nile Red (Sigma–Aldrich) in phosphate-buffered saline (PBS). Samples were observed under a Leica MZ16 F Fluorescence stereomicroscope. The amount of triacylglyceride was measured as described previously [19]. Briefly, ten adult flies were homogenized in 0.1% Tween 20, heated for 5 min at 70 °C, and centrifuged for 3 min at 5500×*g* at 4 °C. The amount of triglyceride was quantified using a Serum Triglyceride Determination Kit (TR0100; Sigma–Aldrich). The triacylglyceride level was normalized to protein concentration. The experiments were carried out in at least triplicate.

2.7. Lifespan and climbing activity

The lifespan of flies was determined as described previously [20]. Newly eclosed flies were kept in a glass vial containing food at 25 °C, transferred to new vials with food every 2–3 days, and the number of dead flies was counted at the time of transfer. For each genotype, at least 100 flies were used for one assay. The climbing activity assay was performed as described previously [21]. Fifteen flies were placed in a graduated cylinder (2 cm in diameter; 20 cm in length), and bumped down to the bottom. Pictures were taken 18 s later, and used to measure the distance that each fly had climbed up the cylinder. Ten trials were performed to determine the average climbing activity.

2.8. Acridine orange staining

Acridine orange staining was performed as described previously [22]. Briefly, the central nervous system of L3 larvae was dissected in PBS. The samples were incubated in 0.5 μg/ml acridine orange (Sigma–Aldrich) in PBS for 5 min at room temperature and rinsed briefly with PBS several times. Samples were observed under a Leica MZ16 F fluorescence stereomicroscope.

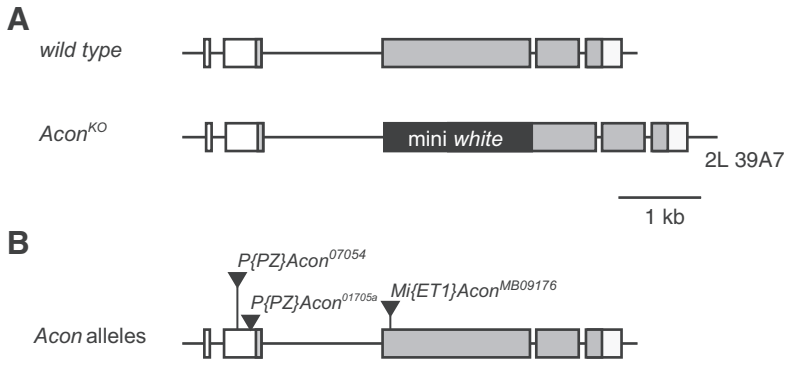

Fig. 1. Schematic representations of the *Acon* locus for wild-type, *Acon*^{KO} (A), and transposon insertion alleles of *Acon* (B). Untranslated regions and protein-coding regions are indicated by white and gray boxes, respectively. Triangles indicate the insertion sites of the transposons.

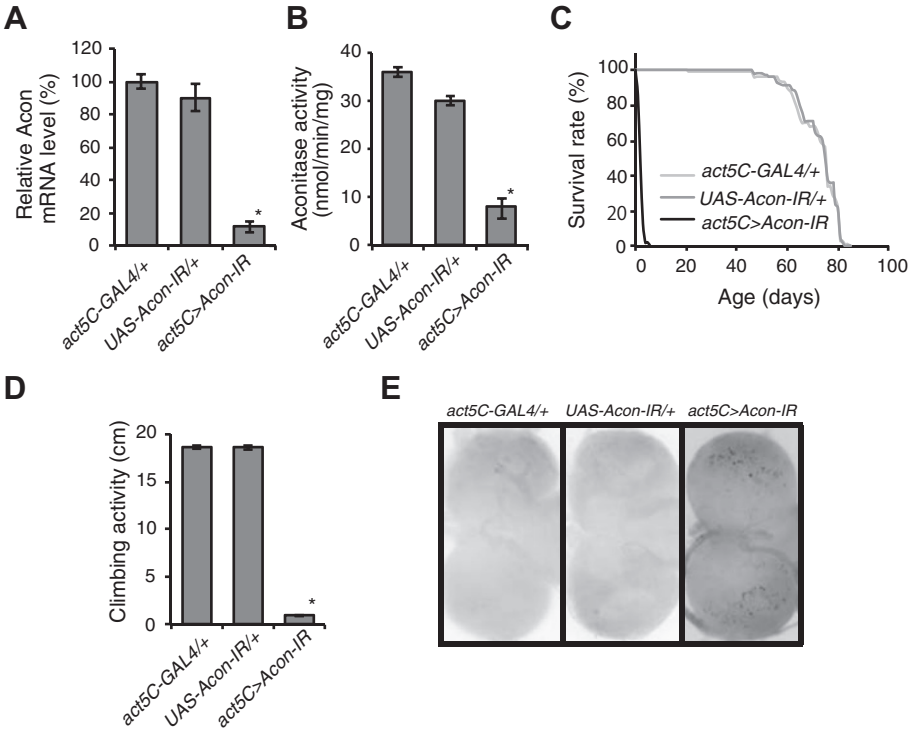

Fig. 2. Phenotypic characterization of *Acon*-knockdown flies. Real-time PCR analysis of *Acon* mRNA in *Acon*-knockdown (*act5C > Acon-IR*) and control flies (*act5C-GAL4/+*, *UAS-Acon-IR/+*) (A). Aconitase activity in mitochondrial fractions from *Acon*-knockdown and control flies (B). Survival curves of *Acon*-knockdown and control flies (log-rank test; $p < 0.001$) (C). Climbing activity of *Acon*-knockdown flies and control flies (D). Representative images of acridine orange-stained larval brains (E). Data represent the mean ± SEM of at least three experiments (*t*-test, $^{*}p < 0.01$).

3. Results and discussion

3.1. Aconitase genes in the Drosophila genome

The *Drosophila melanogaster* genome contains two genes encoding homologs of *m*-aconitase—*Acon* and *CG4706*—which are located on the second and the third chromosome, respectively. The predicted protein sequence of Acon shows 71.7% identity and 82.7% similarity to the human m-aconitase ACO2; CG4706 has slightly lower homology to its human counterpart at 62.8% identity and 72.1% similarity. Unlike the *Acon* gene, which consists of four exons and is expressed ubiquitously, the *CG4706* gene consists of a single exon and is mainly expressed in the testis. It is thought that *CG4706* arose through reverse transcription of *Acon* mRNA during evolution [23]. RT-PCR analyses revealed that *Acon* was expressed throughout development (Supplementary Fig. 1), indicating that *Acon* is the major *m*-aconitase in somatic cells in *Drosophila*.

3.2. Acon is essential for survival

To assess the function of *Acon* in vivo, we first generated *Acon*-deficient flies using gene targeting. The *Acon* region encoding the substrate-binding site was replaced by the *Drosophila* mini-white gene by homologous recombination (Fig. 1A). *Acon*^{ko} homozygous flies were embryonic lethal, suggesting that *Acon* is essential for viability. We also examined the phenotype of three transposon insertion alleles of *Acon*: *P{PZ}Acon*^{07054}, *P{PZ}Acon*^{01705a}, and *Mi{ET1}Acon*^{MB09176} (Fig. 1B). We found that they were all homozygous lethal, and none complemented *Acon*^{ko}. These results strongly support that *Acon* is essential for survival in *Drosophila*.

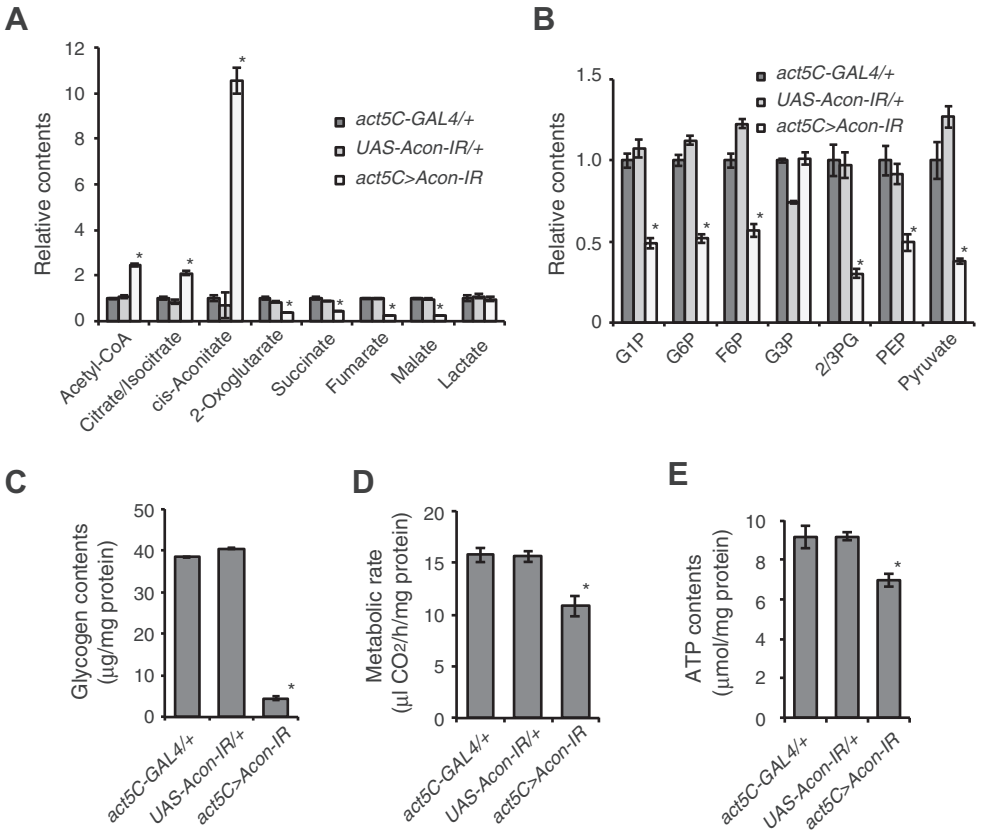

Fig. 3. Metabolomic analysis of *Acon*-knockdown flies. TCA cycle (A) and glycolysis (B) metabolites in *Acon*-knockdown (*act5c > Acon-IR*) and control flies (*act5C-GAL4/+*, *UAS-Acon-IR/+*) were determined by LC-MS-based metabolomic analysis. G1P: glucose 1-phosphate, G6P: glucose 6-phosphate, F6P: fructose 6-phosphate, G3P: glyceraldehyde 3-phosphate, 2/3-PG: 2/3 phosphoglycerate, PEP: phosphoenolpyruvate. Glycogen content of *Acon*-knockdown and control flies (C). Metabolic rate as estimated by CO_2 production (D). ATP content in *Acon*-knockdown and control flies (E). Data represent the mean ± SEM of at least three experiments (*t*-test, $^{*}p < 0.05$).

3.3. Phenotypic characterization of Acon-knockdown flies: lifespan, locomotor activity, and neuronal cell death

Heterozygosity of *Acon* null mutations did not cause any obvious phenotypic changes. Therefore, to explore the in vivo function of *Acon*, we performed RNAi-mediated gene knockdown using *Acon* RNAi lines *P{GD1348}v11767*, *P{GD1348}v12455*, and *P{UAS-Acon.IR}102*. We used *act5C-GAL4* as a driver to knock down *Acon* ubiquitously. *Acon*-knockdown flies exhibited severe phenotypes including lethality. Among the three lines, *P{GD1348}v12455* showed the mildest phenotype; thus, we used this line for further characterization. In addition, we used female flies, since they were more viable than males when *Acon* was knocked down. Quantitative PCR revealed that *Acon* mRNA levels were dramatically reduced in the RNAi-generated *Acon*-knockdown flies (*act5c > Acon-IR*), to about 10% of control levels (*act5C-GAL4/+* or *UAS-Acon-IR/+*) (Fig. 2A). We measured the aconitase enzymatic activity in the mitochondrial fraction isolated from control and *Acon*-knockdown female flies, and found that it was greatly decreased in the knockdown flies, to about 25% of control levels (Fig. 2B). This indicated that RNAi effectively knocked down the *Acon* gene and that these flies would be useful to explore the in vivo effects of defective *m*-aconitase.

First, we measured the lifespan of the *Acon*-knockdown flies. The mean lifespan of *Acon* knockdown flies was much shorter (2.5 ± 0.4 days) than that of control flies (72.2 ± 2.9 days for *act5c/+* and 73.0 ± 2.5 days for *Acon-IR/+*) (Fig. 2C). We next performed a climbing assay to measure locomotor activity. The climbing activity of *Acon*-knockdown flies was dramatically reduced (0.9 ± 0.1 cm) compared with control flies (18.7 ± 0.2 cm for *act5c/+* and 18.6 ± 0.2 cm for *Acon-IR/+*) (Fig. 2D).

It has been reported that a mutation in the human *m*-aconitase gene *ACO2* causes infantile cerebellar-retinal degeneration [12]. Therefore, we examined whether reduction of *Acon* induces cell death in the *Drosophila* larval brain. We found that the number of acridine orange-positive cells was clearly increased in *Acon*-knockdown animals (Fig. 2E), suggesting that Acon activity is crucial for neuronal survival. Because all these knockdown phenotypes were reverted by simultaneous overexpression of *Acon* (Supplementary Fig. 2), we concluded that reduction of *Acon* was responsible for these phenotypes.

3.4. Metabolomic phenotypes of Acon-knockdown flies

m-Aconitase catalyzes the stereo-specific isomerization of citrate to isocitrate via *cis*-aconitate in the TCA cycle, the major energy metabolic pathway in aerobic organisms. We thought that *Acon*-knockdown flies might have defects in energy metabolism, because altered metabolic enzyme activities often cause accumulation or depletion of intermediary metabolites. We measured the content of glycolysis and TCA cycle metabolites using LC-QTofMS. We found that the *Acon*-knockdown flies contained high levels of *cis*-aconitate, the major substrate for aconitase, while most other TCA cycle metabolites, including 2-oxoglutarate, succinate, fumarate, and malate, were significantly decreased (Fig. 3A). There was an increase in the level of acetyl-CoA, which is a substrate in the formation of citrate to initiate the TCA cycle (Fig. 3A). These results indicate that the TCA cycle is impaired in the *Acon*-knockdown flies.

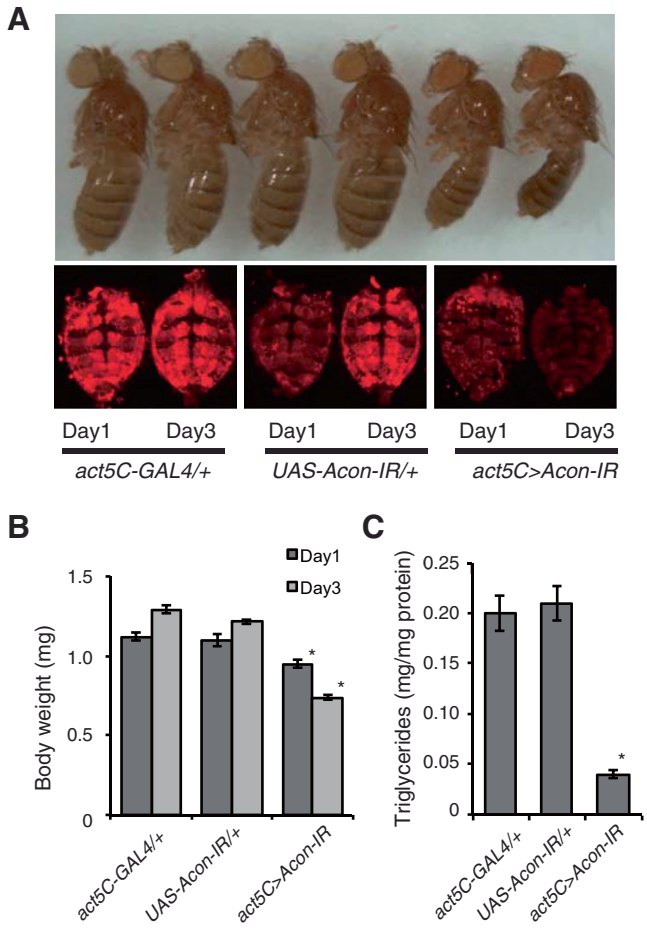

Fig. 4. Rapid loss of body weight and lipid storage in *Acon*-knockdown flies. Body shapes of *Acon*-knockdown and control flies (A, upper panel). Fat bodies in adult abdomens were stained with nile red (A, lower panel). Comparison of body weight (B) and triacylglyceride content (C) between *Acon*-knockdown and control flies. Data represent the mean ± SEM of at least three experiments (*t*-test, $^{*}p < 0.05$). (For interpretation of color in this figure, the reader is referred to the web version of this article.)

In addition, intermediate metabolites of glycolysis (glucose 1-phosphate, glucose 6-phosphate, fructose 6-phosphate, glyceraldehyde 3-phosphate, 2-phosphoglycerate, 3-phosphoglycerate, phosphoenolpyruvate, and pyruvate) were significantly decreased in the *Acon*-knockdown flies (Fig. 3B). Moreover, the level of glycogen was significantly lower in the *Acon*-knockdown flies than in the controls. This suggests that glycolysis is active in the *Acon*-knockdown flies but, because of their defective TCA cycle, they store less glycogen.

The glycolysis and TCA cycle dysfunction in the *Acon*-knockdown flies could affect their metabolic rate. We quantified CO_2 production and the ATP content of the *Acon*-knockdown flies. The *Acon*-knockdown flies produced significantly lower levels of CO_2 compared with control flies (Fig. 3C), implying that the knockdown flies exhibit a decreased metabolic rate. ATP content was also decreased in the *Acon*-knockdown flies (Fig. 3D), suggesting that the aconitase dysfunction directly affects downstream oxidative phosphorylation.

3.5. Lipid metabolism in the Acon-knockdown flies

We noticed that *Acon*-knockdown flies quickly lost weight (Fig. 4A, upper panels) and the average body weight rapidly decreased with age (Fig. 4B). In *Drosophila*, neutral fats such as triacylglycerides are stored in a primary energy storage tissue, called a fat body. We stained fat bodies with Nile Red, a lipophilic stain to visualize lipids. The amount of Nile Red-positive tissue was greatly decreased in the *Acon*-knockdown flies within three days after eclosion (Fig. 4A, lower panels). Consistent with this observation, triacylglyceride levels were significantly decreased in *Acon*-knockdown flies compared with control flies (Fig. 4C). Taken together, these results suggest that *Acon*-knockdown flies utilize lipid as an energy source because of their impaired glycolysis and TCA cycle. A high level of acetyl-CoA in the *Acon*-knockdown flies (Fig. 3A) may be the result of active fatty acid oxidation and dysfunction of the TCA cycle.

In conclusion, we established an *m*-aconitase dysfunction model in *Drosophila* by RNAi-mediated gene knockdown, and demonstrated that the reduced aconitase activity impaired glycolysis and the TCA cycle, and reduced ATP production. *Acon*-knockdown flies showed reduced locomotor activity, a shortened lifespan, and increased cell death in the brain; these phenotypes are also observed in humans with a mutation in *m*-aconitase. The *Acon*-knockdown flies should be useful for investigation of the molecular pathophysiology of *m*-aconitase deficiency.

Acknowledgments

We thank the Drosophila Genetic Resource Center, Kyoto, the Bloomington Stock Center, and the Vienna *Drosophila* RNAi Center for providing stocks. This work was supported by a special Grant from the Tokyo Metropolitan Government to T.A. The sponsor played no role in the study design; in the collection, analysis, or interpretation of the data; in the writing of the report; or in the decision to submit the article for publication.

Appendix A. Supplementary data

Supplementary data associated with this article can be found, in the online version, at http://dx.doi.org/10.1016/j.bbrc.2013.02.040.

References

[1] H.A. Krebs, J.M. Lowenstein, The Tricarboxylic acid cycle, in: D.M. Green (Ed.), Metabolic Pathways, vol., 1, Academic Press, New York, 1960, pp.129–203.
[2] I.A. Rose, E.L. O'Connell, Mechanism of aconitase action. I. The hydrogen transfer reaction, J. Biol. Chem. 242 (1967) 1870–1879.
[3] J.J. Villafranca, A.S. Mildvan, The mechanism of aconitase action. I. Preparation, physical properties of the enzyme, and activation by iron (II), J. Biol. Chem. 246 (1971) 772–779.
[4] M.J. Gruer, P.J. Artymiuk, J.R. Guest, The aconitase family: three structural variations on a common theme, Trends Biochem. Sci. 22 (1997) 3–6.
[5] W.H. Tong, T.A. Rouault, Metabolic regulation of citrate and iron by aconitases: role of iron-sulfur cluster biogenesis, Biometals 20 (2007) 549–564.
[6] D. Cantu, J. Schaack, M. Patel, Oxidative inactivation of mitochondrial aconitase results in iron and H2O2-mediated neurotoxicity in rat primary mesencephalic cultures, PLoS One 4 (2009) e7095.
[7] D. Cantu, R.E. Fulton, D.A. Drechsel, M. Patel, Mitochondrial aconitase knockdown attenuates paraquat-induced dopaminergic cell death via decreased cellular metabolism and release of iron and H(2)O(2), J. Neurochem. 118 (2011) 79–92.
[8] L.J. Yan, R.L. Levine, R.S. Sohal, Oxidative damage during aging targets mitochondrial aconitase, Proc. Natl. Acad. Sci. USA 94 (1997) 11168–11172.
[9] N. Das, R.L. Levine, W.C. Orr, R.S. Sohal, Selectivity of protein oxidative damage during aging in *Drosophila melanogaster*, Biochem. J. 360 (2001) 209–216.
[10] C.S. Yarian, R.S. Sohal, In the aging housefly aconitase is the only citric acid cycle enzyme to decline significantly, J. Bioenerg. Biomembr. 37 (2005) 91–96.
[11] C.S. Yarian, D. Toroser, R.S. Sohal, Aconitase is the main functional target of aging in the citric acid cycle of kidney mitochondria from mice, Mech. Ageing Dev. 127 (2006) 79–84.
[12] R. Spiegel, O. Pines, A. Ta-Shma, E. Burak, A. Shaag, J. Halvardson, S. Edvardson, M. Mahajna, S. Zenvirt, A. Saada, S. Shalev, L. Feuk, O. Elpeleg, Infantile cerebellar-retinal degeneration associated with a mutation in mitochondrial aconitase, ACO2, Am. J. Hum. Genet. 90 (2012) 518–523.
[13] K. Ito, W. Awano, K. Suzuki, Y. Hiromi, D. Yamamoto, The Drosophila mushroom body is a quadruple structure of clonal units each of which contains a virtually identical set of neurones and glial cells, Development 124 (1997) 761–771.

[14] Y. Nakai, J. Horiuchi, M. Tsuda, S. Takeo, S. Akahori, T. Matsuo, K. Kume, T. Aigaki, Calcineurin and its regulator sra/DSCR1 are essential for sleep in Drosophila, J. Neurosci. 31 (2011) 12759–12766.

[15] J. Huang, W. Zhou, A.M. Watson, Y.N. Jan, Y. Hong, Efficient ends-out gene targeting in *Drosophila*, Genetics 180 (2008) 703–707.

[16] G.M. Rubin, A.C. Spradling, Genetic transformation of *Drosophila* with transposable element vectors, Science 218 (1982) 348–353.

[17] J. Bischof, R.K. Maeda, M. Hediger, F. Karch, K. Basler, An optimized transgenesis system for *Drosophila* using germ-line-specific ϕC31 integrase, Proc. Natl. Acad. Sci. USA 104 (2007) 3312–3317.

[18] K. Takeuchi, Y. Nakano, U. Kato, M. Kaneda, M. Aizu, W. Awano, S. Yonemura, S. Kiyonaka, Y. Mori, D. Yamamoto, M. Umeda, Changes in temperature preferences and energy homeostasis in dystroglycan mutants, Science 323 (2009) 1740–1743.

[19] Y. Kishita, M. Tsuda, T. Aigaki, Impaired fatty acid oxidation in a *Drosophila* model of mitochondrial trifunctional protein (MTP) deficiency, Biochem. Biophys. Res. Commun. 419 (2012) 344–349.

[20] M. Tsuda, T. Kobayashi, T. Matsuo, T. Aigaki, Insulin-degrading enzyme antagonizes insulin-dependent tissue growth and Abeta-induced neurotoxicity in *Drosophila*, FEBS Lett. 584 (2010) 2916–2920.

[21] Y. Umeda-Kameyama, M. Tsuda, C. Ohkura, T. Matsuo, Y. Namba, Y. Ohuchi, T. Aigaki, Thioredoxin suppresses Parkin-associated endothelin receptor-like receptor-induced neurotoxicity and extends longevity in *Drosophila*, J. Biol. Chem. 282 (2007) 11180–11187.

[22] M. Tsuda, R. Kawaida, K. Kobayashi, A. Shinagawa, T. Sawada, R. Yamada, K. Yamamoto, T. Aigaki, POSH promotes cell survival in *Drosophila* and in human RASF cells, FEBS Lett. 584 (2010) 4689–4694.

[23] S. Dorus, Z.N. Freeman, E.R. Parker, B.D. Heath, T.L. Karr, Recent origins of sperm genes in *Drosophila*, Mol. Biol. Evol. 25 (2008) 2157–2166.